

Studies on Electrochemical Properties of Polycarbazole Prepared Via Self-Support Polymerization and Self-Doping

S. K. Shakshooki (Corresponding author)

Department of Chemistry, Faculty of Science, University of Tripoli, Libya
Email: shashooki2002@yahoo.com

F. A. El-Akari

Department of Chemistry, Faculty of Science, University of Tripoli, Libya

L. A. Abouderbala

Department of Chemistry, Faculty of Science, University of Tripoli, Libya

A. A. Alahemmer

Department of Chemistry, Faculty of Science, University of Tripoli, Libya

Article History

Received: 1 January, 2023

Revised: 7 March, 2023

Accepted: 24 March, 2023


Published: 30 March, 2023

Copyright © 2023 ARPG

This work is licensed under

the Creative Commons

Attribution International

 CC BY: Creative
Commons Attribution
License 4.0

Abstract

Mixed glassy zirconium-tin phosphate, $g\text{-Zr}_{0.64}\text{Sn}_{0.36}(\text{HPO}_4)_2 \cdot 3\text{H}_2\text{O}$ ($g\text{-ZrSnP}$), nano fibrous cerium phosphate, $\text{Ce}(\text{HPO}_4)_2 \cdot 2,9\text{H}_2\text{O}$ ($n\text{CeP}_f$), and mixed glassy zirconium-tin phosphate / fibrous cerium phosphate nanocomposite membrane, $[g\text{-Zr}_{0.64}\text{Sn}_{0.36}(\text{HPO}_4)_2]_{0.25}[\text{Ce}(\text{HPO}_4)_2]_{0.75} \cdot 4.43\text{H}_2\text{O}$, were prepared and characterized. By chemical, x-ray diffraction (XRD), thermogravimetric analysis (TGA), and Fourier transform spectroscopy (FTIR), Zirconium tin mole ratio were estimated using (EDAX). Novel $[g\text{-Zr}_{0.64}\text{Sn}_{0.36}(\text{HPO}_4)_2]_{0.25}[\text{Ce}(\text{HPO}_4)_2]_{0.75}$ / polycarbazole nanocomposite membrane was prepared via self-support polymerization of carbazole, that was promoted by the reduction of Ce(IV) phosphate present in the inorganic matrix. Possible explanation is $n\text{CeP}_f$ present on the surface of the nanocomposite is attacked by carbazole, converted to cerium (III) orthophosphate (CePO_4). The resultant polycarbazole was characterized by C,H,N analysis, SEM, FT-IR. UV-Vis and electrical conductance measurements. From elemental (C,H,N) analysis, the amount of polycarbazole present in the composite found to be (2.15 % in wt.). Polycarbazole is considered as one of modern material used in solar cells, furthermore it has become an important material for optoelectronic applications in recent years. The dc conductivity of polycarbazole nanocomposite membrane at 28°C (using RC-Circuit) found to be equal to $3 \times 10^{-5} \text{ Scm}^{-1}$, range of semi-conductors. We suggest self-doping occurred on polymerization, which is due to H^+ present in $(\text{O}_3\text{POH})_2$ groups of $[g\text{-Zr}_{0.64}\text{Sn}_{0.36}(\text{HPO}_4)_2]_{0.25}$. The electrochemistry of resultant polycarbazole in acetonitrile solution for a range of concentrations from 1.06×10^{-4} to $2.19 \times 10^{-3} \text{ mol dm}^{-3}$ was carried out using CV techniques. Investigation of its electrochemical properties affords insight into the mechanisms for their oxidation and reduction, therefore provides the basis for evaluating the stabilities of the material and for designing novel polycarbazole-derived materials with desired properties as well as new devices. That will be discussed.

Keywords: Zirconium-tin phosphate; Fibrous cerium phosphate; Polycarbazole; Electrical properties.

1. Introduction

Conducting polymers are a novel class of synthetic metals (called materials of 21st Century) that combine the chemical, electrochemical and mechanical properties of polymers with the electronic properties of metals and semiconductors, generated tremendous interest due to their potential applications in various fields such as rechargeable batteries, electrochromic display devices, separation membranes, sensors and anticorrosive coatings on metal [1, 2], The biggest advantage of conductive polymers is their process ability, low cost, and thermal stability, Kucheldorf, *et al.* [2], Molapo, *et al.* [3], Lu, *et al.* [4]. Their electrical and electrochemical properties show great promise for commercial applications Molapo, *et al.* [3], Sapurina and Shishov [5], Thadathil, *et al.* [6].

Conducting polymers containing nitrogen atoms like polyaniline and polypyrrole, and their substituted derivatives have elicited much interest among researchers because of their reasonably good conductivity, stability, ease of preparation, affordability and redox properties compared to other organic compounds. In particular, the electronic and electrochemical properties of conducting polymers have made them find applications in photovoltaic, Banerjee and Tayagi [7]. Their electrical and electrochemical properties show great promise for commercial applications, Heeger [8], Lange, *et al.* [9], Kucheldorf, *et al.* [2], Zhijiang and Guang [10], Sapurina and Shishov [5]. Conducting polymers are mainly prepared either by chemical oxidative polymerization or electrochemical oxidative polymerization, MacDiarmid, *et al.* [11], Nalwa [1], Chandrasekhar [12], Alemye and Himariam [13], Yang, *et al.* [14]. However, Other methods used for conducting polymers preparations, such as sonication, γ -irradiation, thermal, and microwave are also known, [15].

Polycarbazole and polyindole are less investigated comparing to polyaniline and polypyrrole. Polyindole has similar properties like polyaniline, based on their high conductance and good environmental stability, Chandrasekhar

[12], Grazulevicius, *et al.* [16], Morin, *et al.* [17], Zhijiang and Guang [10], Rejania and Beenab [18]. Kavanoz and Kilic [19], Alem, *et al.* [20], Nayana, *et al.* [21], Lakard, *et al.* [22].

Polycarbazole and its derivatives have excellent optoelectronic properties, high charge carrier mobility and excellent morphological stability which makes them potential candidates in the field of nanodevices, rechargeable batterie, and electro chemical transistors, [21].

Tetravalent metal phosphates(TVMP) are insoluble, posses high ion exchange capacities and very stable toward thermal treatment and wild chemical environment, such as strong acids / bases and redox agents, Albert *etal* [23, 24], Clearfield [25], Shakshooki, *et al.* [26]. They have been known in amorphous and layered forms, Clearfield [25], Shakshooki, *et al.* [26], Alberti, *et al.* [23].

Increase attention direct toward their catalytic, Vecchio, *et al.* [27], electrical conductance, sensors, Alberti, *et al.* [23]. Their layered crystalline materials, resemblance clay minerals, exist as two dimensional (2-D) and three-dimensional (3-D) structures, have the general formulae of α -M(iv)(HPO₄)₂·H₂O, Θ -M(iv)(HPO₄)₂·5H₂O and γ -M(iv).PO₄·H₂PO₄·2H₂O, (where M = Ti, Zr, Hf, Ge, Sn, Ce etc) have been established Clearfield [25], Szirtes, *et al.* [28], Shakshooki, *et al.* [26], Alberti, *et al.* [23]. α -Layered mixed zirconium-titanium phosphates, Zr_xTi_(1-x)(HOP₄)₂·H₂O(α -Zr_xTi_(1-x)P), (0 ≤ x ≤ 1), are known, Shakshooki, *et al.* [26], To date there have been very little work on layered α -zirconium-tin phosphates. However, preparation of mixed α -Zr_xSn_(1-x)(HOP₄)₂·H₂O(α -Zr_xTi_(1-x)P), for 0 ≤ x ≤ 1, via different methods and their characterization have been reported, Barganasco, *et al.* [29], Trobajo and Rodríguez [30], Shakshooki, *et al.* [31].

Crystalline cerium phosphates have been studied for a long time as ion exchangers, their structures remain unknown for some times, [32],[33] Shakshooki, *et al.* [34], Tushato, *et al.* [33], Miguel, *et al.* [32], Miguel, *et al.* [32], The reason is that, the composition, the structure and the degree of crystallinity of their precipitates results from reaction of solutions containing a Ce^{IV} salt mixed with a solution of phosphoric acid of [(PO₄)/ Ce^{IV} ratio], strongly dependent on the experimental conditions such as rate and order of mixing of the solutions, stirring, temperature and digestion time, this also implemented on fibrous cerium phosphate, [33]. To date most of the work on fibrous cerium phosphate was carried out on its ion exchange and intercalation Romano and Alves [35], electrical conductance properties Casciola, *et al.* [36], and as self-support polymerization Shakshooki *et al.* [31, 34].

Electrochemistry is the branch of chemistry that deals with the relationship between electricity and chemical reaction, Hamann, *et al.* [37], Hibbert [38]. Others have defined it as the science of the interaction of phases containing electrons and phases containing ions. Typically, it involves the transfer of the electrons between the solution and the electrode surface. This transfer plays a pivotal role in determining the outcome of a chemical reaction. Furthermore, electrochemistry through cyclic voltammetry techniques offers a powerful approach to examine an electrochemical properties of carbzole in acetonitrile solutions.

2. Materials and Methods

2.1. Chemicals

Ce(SO₄)₂·4H₂O of (Merck), ZrOCl₂·8H₂O, SnCl₄ and H₃PO₄ (85%) of (BDH), polycarbazole, dimethyl sulfoxide and CH₃CN of (Reidel de-Hean) Tetrabutyl ammonium- hexaflouro phosphate (TBAPF₆) of (Fluka),. Other reagents used were of analytical grade.

2.2. Instruments used for Analysis

X-ray powder diffractometry Siemens D-500, using Ni-filtered CuK_α (λ= 1.54056Å), TG/DTA SII Extra 6000 Thermogram,

TG/DTA Perkin-Elmer SII,

Scanning electron microscopy (SEM) Jeol SMJ Sm 5610 LV,

Transmission electron microscopy (TEM) Zeiss TEM 10 CR,

Fourier Transform IR spectrometer, FT-IR-6100,

CHN Elemental analyzer-Germany,

pH Meter WGW 521

UVVis Spectrometero photometer. Perki Elmir.

CV's were recorded using e DAQ potentiostat, 466 System (Model ER466)

For electrochemical measurements The background electrolyte Tetrabutyl ammonium- hexaflouro phosphate (TBAPF₆), (Fluka) was used. A stock solution (100 mmol dm⁻³) was prepared by weighing the appropriate amount of this compound and dissolved it in dry CH₃CN., The prepared solution were de-aerated and stored under Argon gas.

2.3. Preparation of Nanofibrous Cerium Phosphate

300ml of 0.05M CeSO₄·4H₂O in 0.5M H₂SO₄ solution were added drop wise to 300ml of 6M H₃PO₄ at 80°C with stirring. After complete addition the resultant material left to digest at that temperature for 4h. To that one liter of hot distilled water, (~60°C), was added with stirring for 1h. The resultant slurry aqueous solution of nanofibrous cerium phosphate, then was kept.

2.4. Preparation of Glassy Mixed Zirconium-tin Phosphate

Reaction of a mixture of 135 ml 0.5M ZrOCl₂·8H₂O and 65 ml 0.5M SnCl₄ in 4M HCl with 240ml of 12% H₃PO₄ at room temperature (25°C) with stirring for 1h. The resultant product was aged in mother liquor for 24h, and

then was filtered on Buchner funnel to obtain the wet gel of mixed zirconium tin phosphate. , 90 grams of the wet gel were subjected to dry in oven at 60°C for 24h. The resultant dried material was cracked with distilled water, filtered washed once with distilled water to obtain glassy $Zr_{0.64}Sn_{0.36}(HPO_4)_2 \cdot 3H_2O$, with visual vitreous look.

2.5. Preparation of Glassy Mixed Zirconium.-Tin Phosphate.-Fibrous Cerium Phosphate / Polycarbazole Nanocomposite Membrane

0.25g of $[g-Zr_{0.64}Sn_{0.36}(HPO_4)_2]_{0.25}[Ce(HPO_4)_2]_{0.75} \cdot 4.43H_2O$ sheet was immersed in 17ml 4% carbazole in acetone, left static for 72h at room temperature. It was observed with time the color changes gradually to (light green and finally to green). The impregnated sheet was removed and washed with acetone, left to dry in air. Electrical conductivity measurement of $[g-Zr_{0.64}Sn_{0.36}(HPO_4)_2]_{0.25}[Ce(HPO_4)_2]_{0.75}$ / polycarbazole composite The dc conductivity (Scm^{-1}) of the polycarbazole composite resultant conducting polymer nanocomposite membrane were measured on compact pellets at (28°C) by RC-Circuit., mass 9.4mg of gridding sample pressed under 1.0ton pressure, using carbon black electrodes.

2.6. Electrochemistry of Carbazole

Electrochemistry of three electrode system was carried out for carbazole in CH_3CN using CV techniques. It was performed in ordinary specimen tube (25 x 50 mm) with the auxiliary, reference and working electrodes placed through holes in the plastic cap. Air was excluded by bubbling Argon into the sample. The reference electrode was placed close to the working electrode. The distance between the working electrode and auxiliary electrode was also kept small to minimise the compliance voltage. It worth mentioned that, in this work we used the Ag/Ag_2O electrode. It is a novel electrode that has advantages over calomel electrode [Kissinger and Heineman \[39\]](#). It avoids sample contamination with water and it allows the reference compartment to have the same solution as the sample minimising liquid junction effect, ($Ag/AgCl$ and Ag/Ag^+).

The electrochemical properties of carbazole, were studied using voltammetric technique. Solutions of different concentrations of the compound in CH_3CN were subjected to record their CV's at different scan rates using EChem software.

3. Results and Discussion

Mixed glassy zirconium-tin phosphates, $Zr_{0.64}Sn_{0.36}(HPO_4)_2 \cdot 3H_2O$ and nano fibrous cerium phosphate, $Ce(HPO_4)_2 \cdot 2,9H_2O$, were characterized by x-ray diffraction (XRD), thermogravimetric analysis (TGA), and by Fourier transform spectroscopy (FT-IR), zirconium tin mole ratio were estimated using (EDAX).

3.1. XRD of Glassy Mixed $Zr_{0.64}Sn_{0.36}(HPO_4)_2 \cdot 3H_2O$

[Figure \(1\)](#) shows x-ray diffraction of glassy, $Zr_{0.64}Sn_{0.36}(HPO_4)_2 \cdot 3H_2O$, characteristic of amorphous type of $M(IV)$ phosphates. The XRD does not consist of any peaks.

3.2. EDAX of Glassy Mixed $Zr_{0.64}Sn_{0.36}(HPO_4)_2 \cdot 3H_2O$

Estimation of % ratio of Zr:Sn in glassy mixed $Zr_{0.64}Sn_{0.36}(HPO_4)_2 \cdot 3H_2O$, carried out by EDAX. The results are given in [Figure \(2\)](#), accordingly the products were formulated.

Figure-1. XRD of $g-Zr_{0.64}Sn_{0.36}(HPO_4)_2 \cdot 3H_2O$

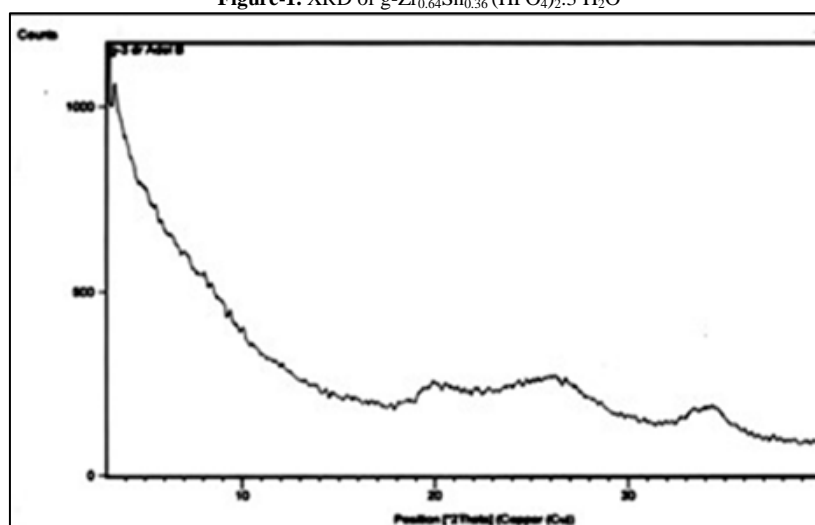
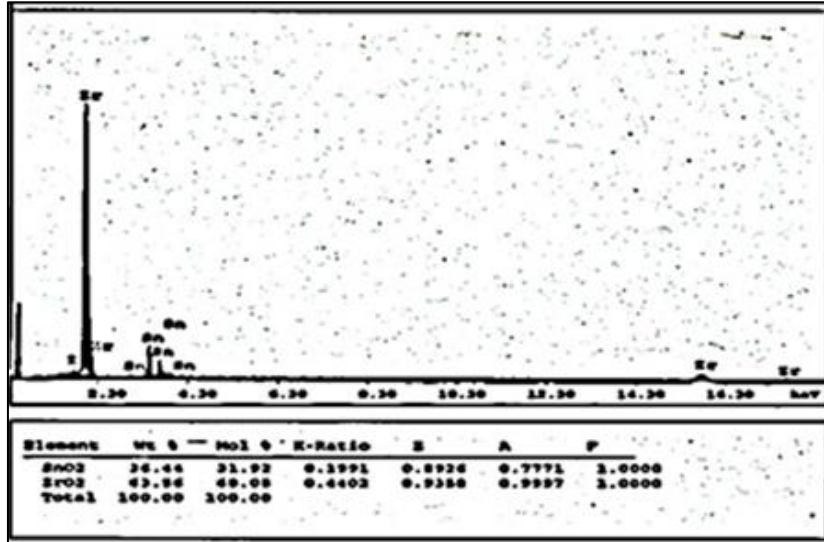


Figure-2. % ratio of - Zr_{0.64}Sn_{0.36}(HPO₄)₂.3H₂O

3.3. FT-IR Spectrum of Glassy Mixed Zr_{0.64}Sn_{0.36}(HPO₄)₂.3H₂O

Figure (3), shows infrared spectrum of g-Zr_{0.64}Sn_{0.36}(HPO₄)₂.3H₂O were recorded in KBr pellet medium. The IR spectrum shows broad bands at 3590cm⁻¹ and 2350cm⁻¹ are due to OH groups of interstitial water (or free water) symmetric-asymmetric stretching vibration, respectively. The sharp band at about 1630 cm⁻¹ is due to H-O-H bending. Broad band in the region 850-1300-850cm⁻¹ is due to mixing of group vibrations in the range P=O (Hydrogen bonded), P-OH and P-O-P groups, respectively. Weak absorption bands at 600 cm⁻¹, and 520cm⁻¹ can be assigned to P-O, Sn-O and Zr-O vibrations.

3.4. TGA of Glassy Mixed Zr_{0.64}Sn_{0.36}(HPO₄)₂.3H₂O

Figure (4) shows the TGA of glassy mixed Zr_{0.64}Sn_{0.36}(HPO₄)₂.3H₂O. were carried out in the range 30-1000°C. The thermal decomposition found to occur in two stages. The first stage is due to the loss of water of hydration up to about 200°C. The second stage is due to the loss of the structural water, which a result of (POH) groups condensation. The final product was [Zr_{0.64}Sn_{0.36}]P₂O₇.

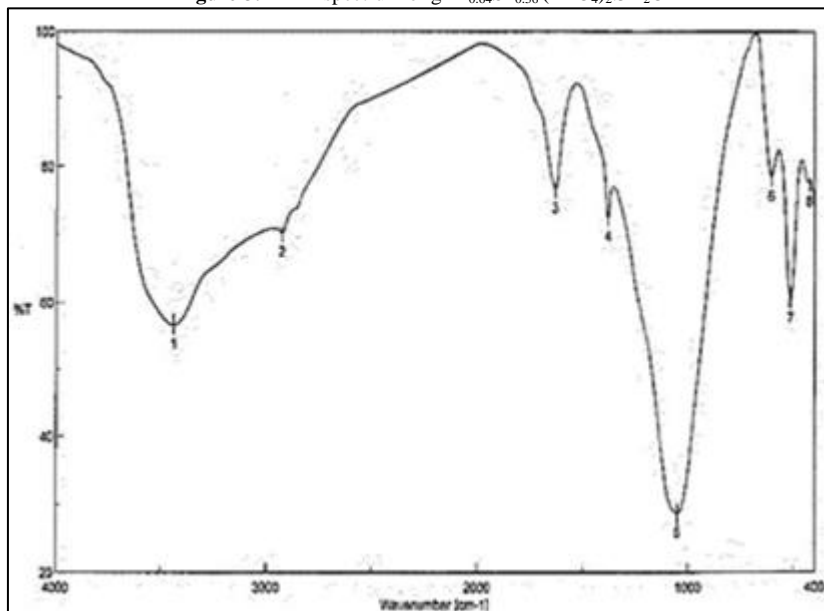
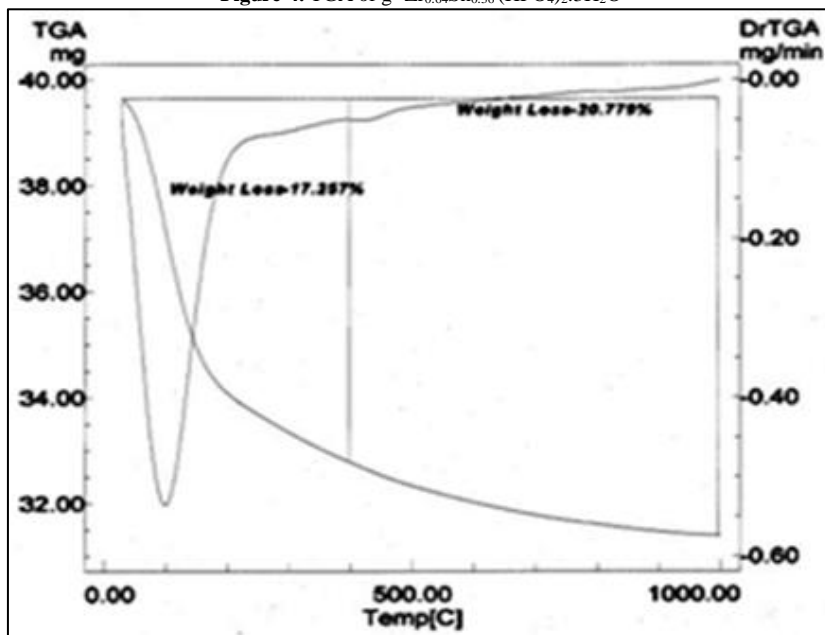
Figure-3. FT-IR spectrum of g-Zr_{0.64}Sn_{0.36}(HPO₄)₂.3H₂O

Figure-4. TGA of g- $Zr_{0.64}Sn_{0.36}(HPO_4)_2 \cdot 3H_2O$ 

Nanofibrous cerium phosphate membrane, $Ce(HPO_4)_2 \cdot 2.9H_2O$ ($nCeP_f$), was prepared and characterized by chemical analysis, XRD, TGA, FT-IR, scanning electron microscope (SEM) and transmission electron microscopy (TEM).

3.5. XRD and FT-R of $nCeP_f$

XRD of ($nCeP_f$) is shown in Figure (5), with $d_{001} = 10.89\text{\AA}$. Its thermogram of is shown in Figure (6). The thermal decomposition occurs in continuous process, The thermal analysis was carried out at temperatures between 10-775°C, the final product was CeP_2O_7 . Loss of water of hydration occurs between 60-200°C, followed by POH groups condensation. The total weight loss found to be equal to 19.09%.

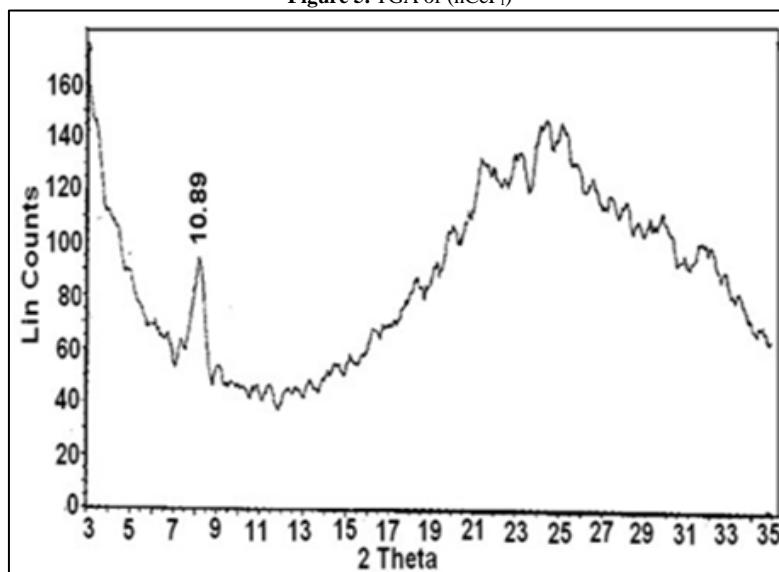
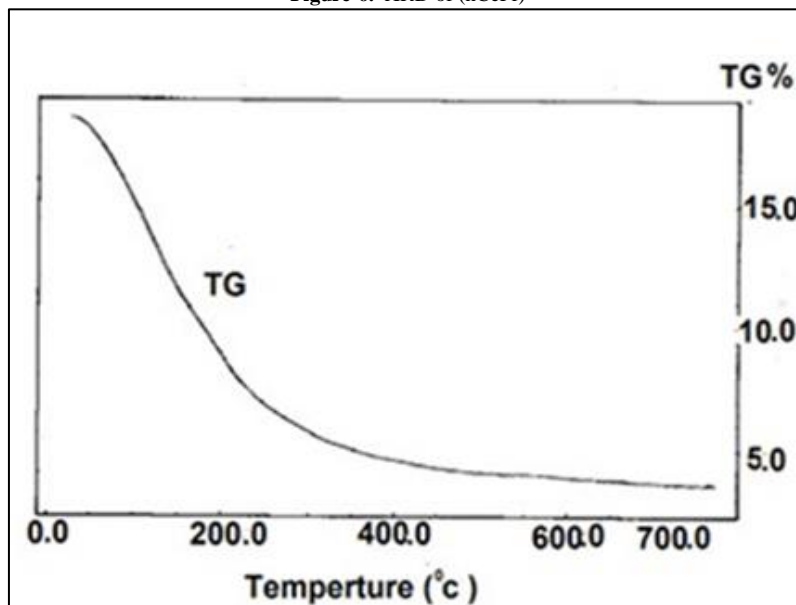
Figure 5. TGA of ($nCeP_f$)

Figure-6. XRD of (nCePf)



3.6. FT-IR and SEM of nCeP_f

Figure (7), shows FT-IR spectrum of nano fibrous $\text{Ce}(\text{HPO}_4)_2 \cdot 2.9\text{H}_2\text{O}$, with a trend similar to that of M(IV) phosphates. It consists of broad band centered at 3350cm^{-1} is due to OH groups symmetric stretching of H_2O , small sharp band at 1628cm^{-1} is related to H-O-H bending, and sharp broad band centered at 1045cm^{-1} is corresponds to phosphate groups vibration. The bands at the region $630\text{-}450\text{ cm}^{-1}$ are ascribe the presence of $\delta(\text{PO}_4)$.

Its SEM morphology is shown in Figure (8). The photograph shows its average size is $\sim 20.5\text{ nm}$.

3.7. TEM of nCeP_f

Transmission electron microscopy image (TEM) of the nanosized fibrous cerium phosphate, (2.5% loading in PVA), of fibrous visual look, is shown in Figure (9). The photograph shows its average size is $\sim 15\text{ nm}$.

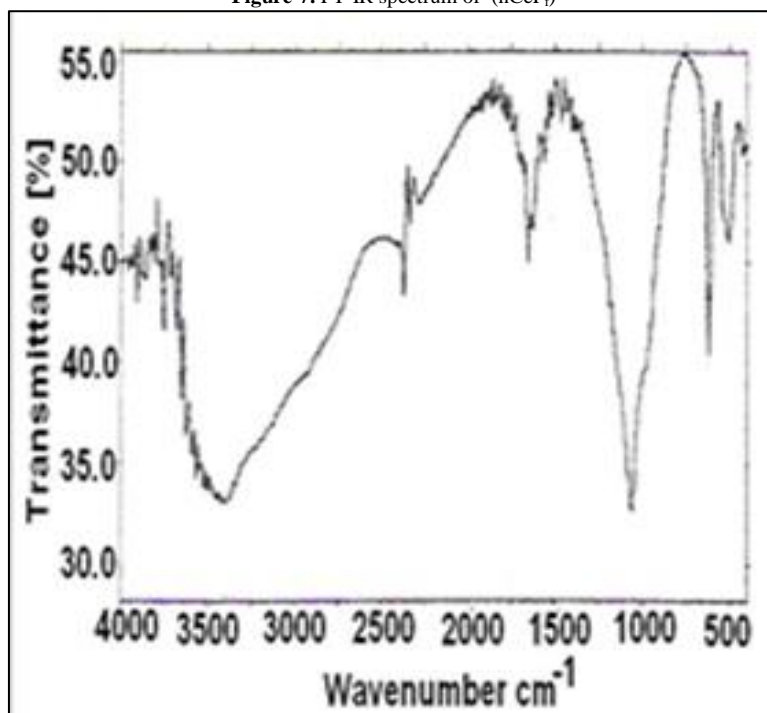
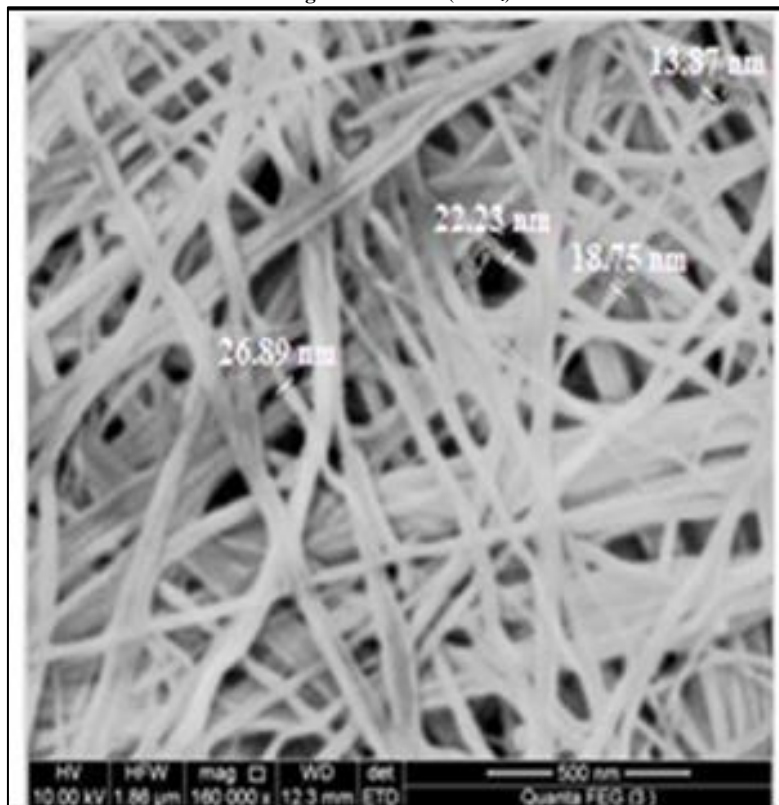
Figure-7. FT-IR spectrum of (nCeP_f)

Figure-8. SEM of (nCeP_f)Figure-9. TEM of (nCeP_f)

3.8. Ion Exchange Capacity

The ion exchange capacity of nanosized fibrous cerium(IV) phosphate, $\text{Ce}(\text{HPO}_4)_2 \cdot 2.9\text{H}_2\text{O}$, found to be equal to 5.21 meq/g.

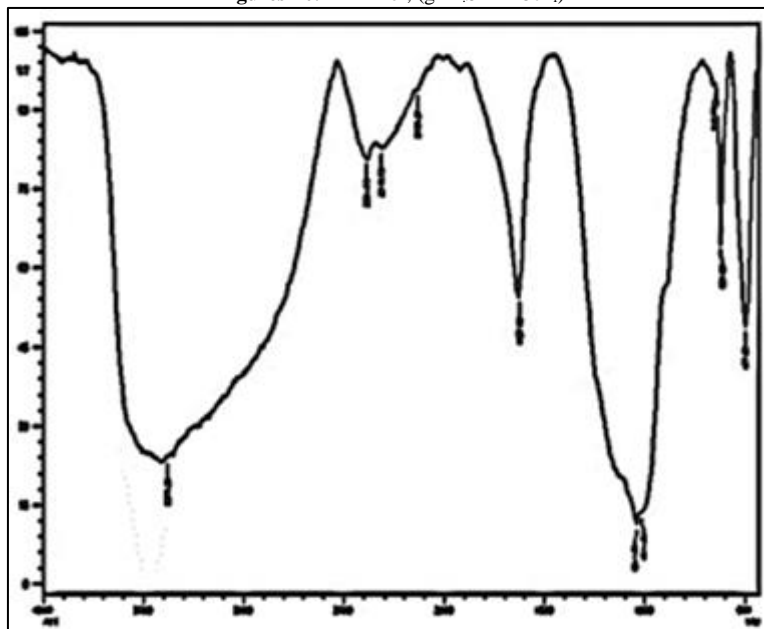
Novel glassy mixed zirconium-tin phosphates fibrous cerium phosphate nanocomposite membrane $[\text{g-Zr}_{0.64}\text{Sn}_{0.36}(\text{HPO}_4)_2]_{0.25} [\text{Ce}(\text{HPO}_4)_2]_{0.75} \cdot 4.43\text{H}_2\text{O}$, was prepared and characterized by FT-IR spectroscopy, SEM and thermal treatment.

3.9. FT-IR and SEM of Mixed Glassy Zirconium-tin Phosphate.-Fibrous Cerium Phosphate Nanocomposite Membrane

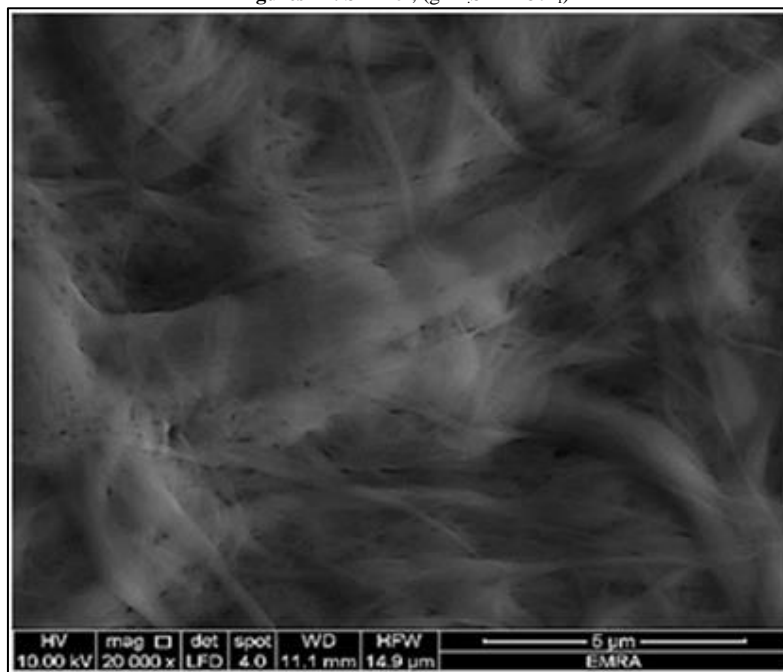
Figure (10) shows FT-IR spectra of composite compound $[g\text{-Zr}_{0.64}\text{Sn}_{0.36}(\text{HPO}_4)_2]_{0.25} [\text{Ce}(\text{HPO}_4)_2]_{0.75} \cdot 4.43\text{H}_2\text{O}$, found to follow the same trend of FT-IR spectra of M(iv) phosphates. were recorded in KBr pellet. It consists of broad band centered at 3425cm^{-1} due to OH groups symmetric-asymmetric stretching-vibration. Small sharp band at 1665cm^{-1} is related to H-O-H bending, sharp broad band centered at 1010cm^{-1} corresponds to phosphate groups vibration.

Figure (11), shows the surface morphology of $[g\text{-Zr}_{0.66}\text{Sn}_{0.34}(\text{HPO}_4)_2]_{0.25} [\text{Ce}(\text{HPO}_4)_2]_{0.75} \cdot 4.43\text{H}_2\text{O}$ nanocomposite membrane, (g-Zr,SnP-nCeP_f). The morphology image reveal a uniform distribution of glassy zirconium-tin phosphates over and between fibrous cerium phosphate matrix.

Figures-10. FT-IR of, (g-Zr,SnP-nCeP_f)



Figures-11. SEM of, (g-Zr,SnP-nCeP_f)



The formation of the polycarbazole nanocomposite results from the immersion of inorganic sheets into the monomer solution. The resultant nanocomposite membranes were characterized by C,H,N elemental analysis, scanning electron microscopy (SEM), and FT-IR spectroscopy accordingly it was formulated as $[g\text{-Zr}_{0.64}\text{Sn}_{0.34}(\text{HPO}_4)_2]_{0.25} [\text{Ce}(\text{HPO}_4)_2]_{0.75} / \text{polycarbazole}(2.5\% \text{ in wt.})$.

3.10. FT-IR Spectrum and SEM of [g-Zr_{0.66}Sn_{0.34} (HPO₄)₂]_{0.25} [Ce(HPO₄)₂]_{0.75} / Polycarbazole Nanocomposite Membrane

Figure (12) shows typical FT-IR spectrum of [g-Zr_{0.64}Sn_{0.34}(HPO₄)₂]_{0.25}[Ce(HPO₄)₂]_{0.75} /PCz nano composite membrane, consist of broad band centered around ~ 3421 cm⁻¹, is due to OH groups symmetric stretching of H₂O super imposed with the N-H stretching of aromatic amines (expected at the range 3695.9-2924.5cm⁻¹). Small band around ~1630 cm⁻¹ is related to H-O-H bending, and sharp broad band centered at 1000 cm⁻¹ is corresponds to phosphate groups vibration. The bands at range 2200-2019 ascribed for C-H stretching, respectively. Besides, the v,s.band at 1217 cm⁻¹ may be ascribed to the C-H out of plane twisting vibration. Formation of PCz was confirmed by presence of the bands at 1400-1200cm⁻¹ is due to the ring stretching vibrations of carbazole moiety, bands in the range of 700-520 cm⁻¹ attributed to C=C out of plane twisting and vibrations of ring distortion of aromatic structure of PCz moiety.

Figures (13) shows the surface morphology (SEM) of and [n-Zr_{0.64}Sn_{0.36}(HPO₄)₂]_{0.25} [Ce(HPO₄)₂]_{0.75} /PCz nanocomposite membranes reveal a distribution of the polymer over and between the inorganic matrix.

Figure-12. FT-IR spectrum of [g-Zr_{0.64}Sn_{0.36}P - nCeP_i] /PCz

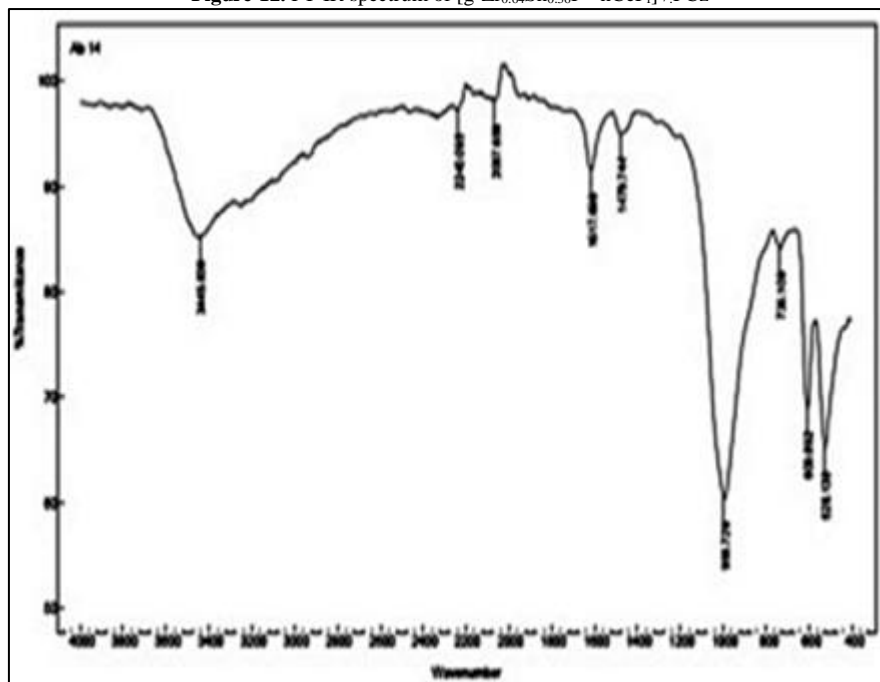
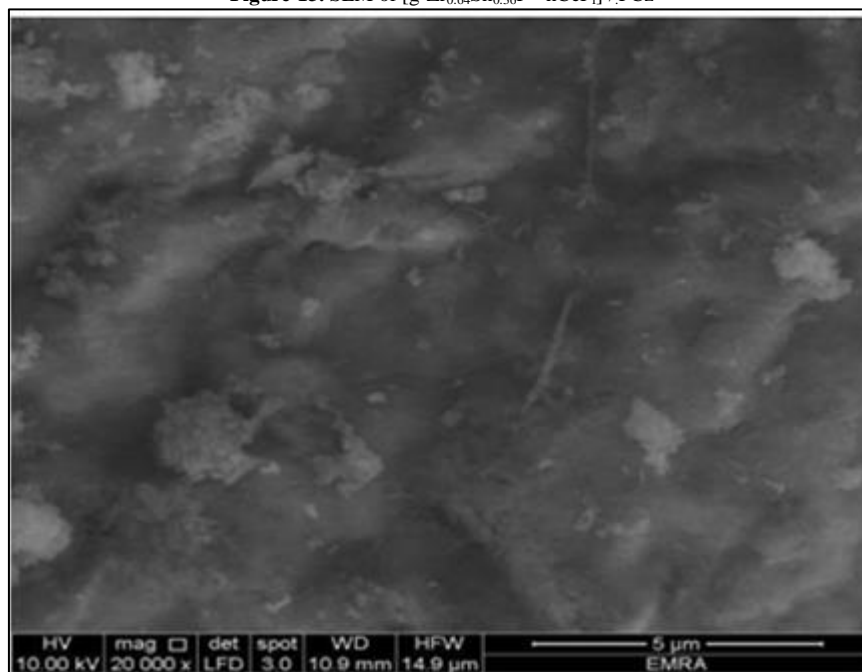
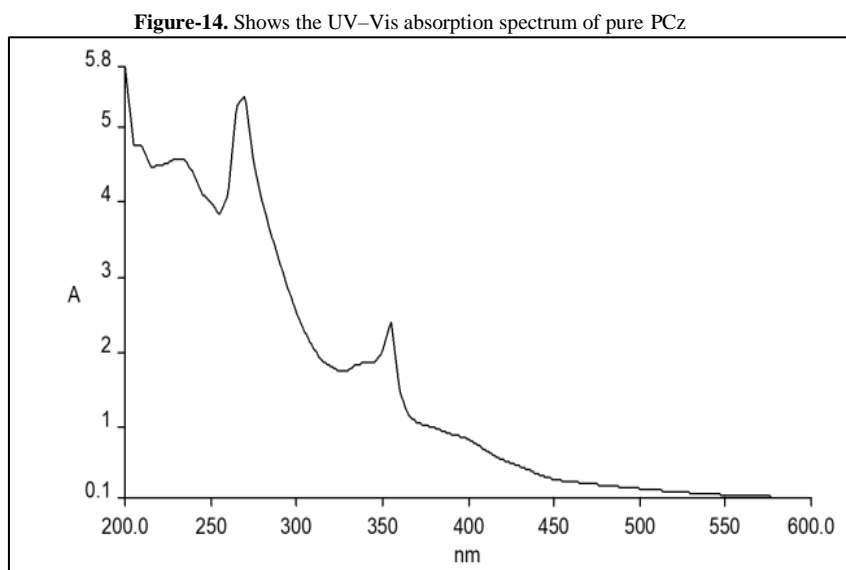


Figure-13. SEM of [g-Zr_{0.64}Sn_{0.36}P - nCeP_i] /PCz



3.11. UV-vis Absorption Spectrum of Pure PCz Results from CH₃CN Treatment of (nZr_{0.73}Sn_{0.27}P_f-CeP_f)/PCz Nanocomposite Membrane

Figure (14) shows the UV-Vis absorption spectrum of pure PCz results from (DMSO-Extract) of (g-Zr_{0.64}Sn_{0.36}P_f-CeP_f)/PCz nanocomposite membrane, CH₃CN treatment. The absorption bands at 270 and 355, for polycarbazole. The two absorptions of the polymer correspond to valence band to conduction band at 270nm, and a polaronic level to π^* conduction band at 355nm, respectively. This confirms the formation of the polymer.



The electrochemical oxidation of carbazole was mathematically calculated from its CV. As can be seen from Figure (15), The compound shows one reversible redox process at which it oxidized at 1.17 V giving an oxidation faradic current of 37.3 μ A, and then reduced at -0.89 V, giving a reduction faradic current of 43.9 μ A. It shows further reduction peak at about -2.34 V. The latter might be indicated to non-reversible electrochemical reduction.

Figure (16) illustrated the comparison of CV's of both the polymer carbazole and the solvent CH₃CN on its own. As can be seen, there is no electrochemical process (as expected) for the solvent in the studied potential range while the polymer shows more than one redox process, as mentioned above.

Figure-15. CV's of solution of Ab8 and the solvent CH₃CN recorded at scan rate of 100 mV/s and at room temperature, using glassy carbon electrode and Ag/AgCl as reference electrode

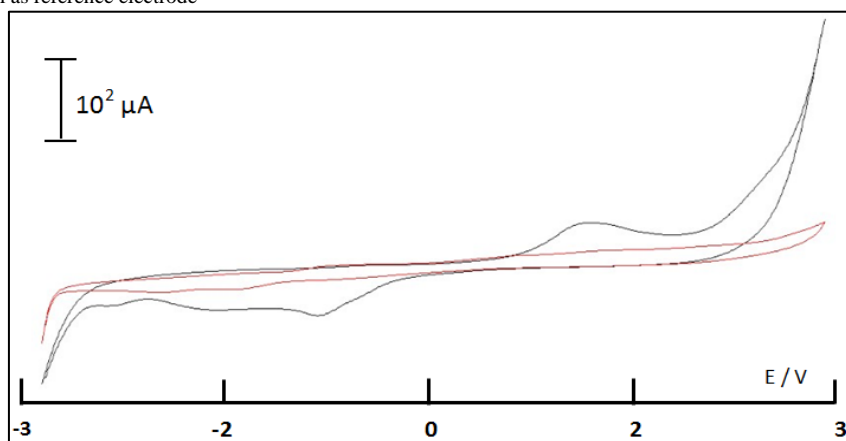


Figure-16. CV of polycarbazole recorded at scan rate of 100 mV/s and at room temperature, using glassy carbon electrode and Ag/AgCl as reference electrode

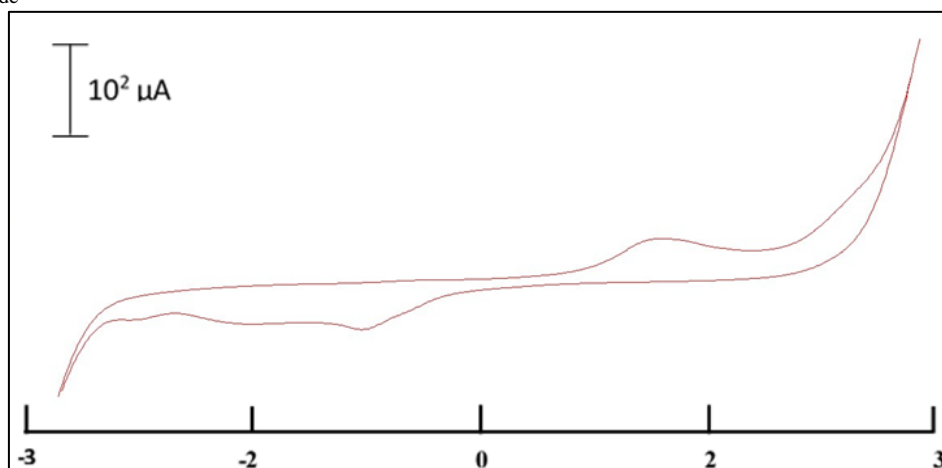
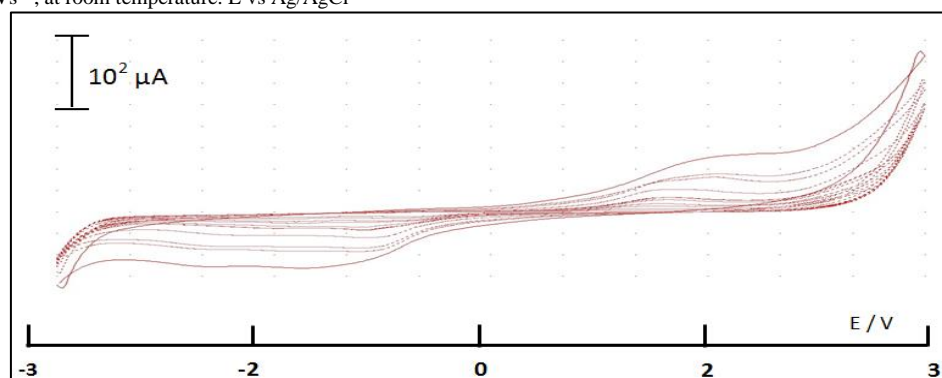


Table 1 summarized the electrochemical parameters of different concentrations of solutions of polycarbazole in CH₃CN. As can be seen from Table 1, there is a significant increment of the oxidation potential value. For example, it was 1.71 V when the concentration 1.06 mole dm⁻³, it became 1.21 V at the concentration of 2.19 mole dm⁻³. This significant increment reflects the shift in the oxidation potential of the polymer. It can be explained in terms of increasing the electron density of the polymer owing to the growth of copolymerization process. Conversely, the small value of the shift has been observed for the reduction potential. It can be attributed to the stability of species that have been oxidized through the forward potential scan.

Table-1. The electrochemical data of the polymer carbazole at scan rate of 100 mV/s E vs Ag/AgCl

Conc.(v/v)	Conc. Mole/dm ⁻³	E _{ox} / V	i _{ox} /μA	E _{Red} / V	i _{Red} / μA
0.25	1.06	1.71	18.925	-0.97	-29.842
0.40	1.87	1.42	33.379	-0.81	-49.020
0.50	2.23	1.25	33.781	-0.88	-41.955
0.60	1.81	1.36	36.625	-0.84	-47.989
0.63	2.23	1.24	37.369	-0.88	-42.912
0.67	2.15	1.36	37.125	-0.85	-45.327
0.73	2.19	1.21	37.555	-0.88	-43.895

Figure-17. Shows the CV's of solution of concentration of 0.32 mole dm⁻³ of Ab₈ in CH₃CN at scan rates of 0.01, 0.02, 0.04, 0.05, 0.08, 0.1, 0.2, 0.4, 0.5 and 1.0 Vs⁻¹, at room temperature. E vs Ag/AgCl



The CV's of the compound at different scan rates show a deviation on both oxidation and reduction potential. These effect is obvious in the voltammograms of the compound that have been illustrated in figure 16. This voltammogram were recorded at scan rates of 0.01, 0.02, 0.04, 0.05, 0.08, 0.1, 0.2, 0.4, 0.5 and 1 V/s. The obvious deviation of redox potential confirmed the existence of reversible electrochemical process of polycarbazole.

4. Conclusion

Mixed glassy zirconium-tin phosphate, Zr_{0.64}Sn_{0.36}(HPO₄)₂·3H₂O(g-ZrSnP), nano fibrous cerium phosphate, Ce(HPO₄)₂·2.9H₂O(nCeP_f), and mixed glassy zirconium-tin phosphate / fibrous cerium phosphate nanocomposite membrane, [g-Zr_{0.64} Sn_{0.36} (HPO₄)₂]_{0.25} [Ce(HPO₄)₂]_{0.75}·4.43H₂O, were prepared and characterized.glassy mixed zirconium- tin phosphate/polycarbazole nanocomposite membrane, [g-Zr_{0.64} Sn_{0.36} (HPO₄)₂]_{0.25}[Ce(HPO₄)₂]_{0.75} / PCz, was prepared via self-support polymerization of carbazole It was characterized by C,H,N analysis, SEM ,FT-IR. UV-Vis and electrical conductance measurements. The dc conductivity of polycarbazole nanocomposite membrane at 28⁰C in DMSO solution, (using RC-Circuit) found to be equal to 3x10⁻⁵ Scm⁻¹, range of semi

conductors. We suggest self-doping occurred on polymerization, which is due to H^+ present in $(O_3POH)_2$ groups of $[g-Zr_{0.64}Sn_{0.36}(HPO_4)_2]$.

The electrochemical study through cyclic voltammetry technique, for both the polymer carbazole and the solvent CH_3CN on its own, shows no electrochemical process for the solvent in the studied potential range while the polymer shows more than one redox process reflects its oxidation and reduction potential and its faradic current. Affords insight into the mechanisms for their oxidation and reduction, therefore provides the basis for evaluating the stabilities of the material and for designing novel polycarbazole-derived materials with desired properties as well as new device.

Acknowledgement

To Department of Chemistry, Faculty of Science, University of Tripoli, for providing facilities for this research.

References

- [1] Nalwa, H. S., 1997. *Handbook of organic conductive molecules and polymers*. UK: John Wiley.
- [2] Kucheldorf, H. R., Luken, O., and Swift, G., 2010. *Hand book of polymer synthesis*. 2nd ed. CRC Press.
- [3] Molapo, K. M., Ndangili, P. M., Ajayi, R. F., Mbambisa, G., Mailu, S. M., Njomo, N., Masikini, M., Baker, P., and Iwuoha, E. I., 2012. "Review : Electronics of conjugated polymers (i): Polyaniline." *Int. J. Electrochem. Sci.*, vol. 7, p. 11859.
- [4] Lu, J., Kololuoma, T., Movileanu, R., and Tao, Y., 2018. "Flexographic printing of polycarbazole-based inverted solar cells. *Org. Electron.*, 52, 146–152. Alemyehe, T. and Himariam, B. (2014), Synthesis and characterization of conducting polymers: A Review Paper." *Int. J. of recent Res. in Phys. and chem. Sci.*, vol. 1, p. 24.
- [5] Sapurina, I. Y. and Shishov, M. A., 2012. *New polymers for special applications*. Ailton De Souza Gomes, Ed.
- [6] Thadathil, A., Pradeep, H., Joshy, D., Ismail, Y. A., and Periyat, P., 2022. "Polyindole and polypyrrole as a sustainable platform for environmental remediation and sensor application." *Mater. Adv.*, vol. 3, pp. 2990-3022.
- [7] Banerjee, S. and Tayagi, A. K. E., 2012. *Functional materials: Preparation, processing and applications*. Elsevier.
- [8] Heeger, A., 2001. "Semiconducting and metallic polymers: The fourth generation of polymeric materials." *Reviews of Modern Phys.*, vol. 73, p. 681.
- [9] Lange, U., Roznyatovskaya, N. V., and Mirsky, V. M., 2008. "Conducting polymers in chemical sensors and arrays." *Analytica Chimica Acta*, vol. 614, pp. 1-26.
- [10] Zhijiang, C. and Guang, Y., 2010. "Synthesis polyindole and its evaluation for Li-ion battery applications." *Synth. Met.*, vol. 160, pp. 1902-1905.
- [11] MacDiarmid, A. G. R. J., Mammone, R. J. R. B., Kaner, R. B., and Porter, L., 1985. "The concept of 'doping' of conducting polymers: the role of reduction potentials." *Royal Society*, vol. 314, p. 1528.
- [12] Chandrasekhar, P., 1999. *Conducting polymers*. London: Kluwer. p. 387.
- [13] Alemyehe, T. and Himariam, B., 2014. "Synthesis and characterization of conducting polymers: A Review Paper." *Int. J. Of Recent Res. in Phys. and Chem. Sci.*, vol. 1, p. 24.
- [14] Yang, J., Liu, Y., S., L., Li, L., Zhang, C., and Liu, T., 2017. "Conducting polymer composites: material synthesis and applications in electrochemical capacitive energy storage." *Material Chemistry*, vol. 1, pp. 251-261.
- [15] Chichester, Namsheer, K., and Chandra, C. S., 2021. "Conducting polymers: a comprehensive review on recent advances in synthesis, properties and applications." *RSC Adv.*, vol. 11, pp. 5659-5697.
- [16] Grazulevicius, J. V., Strohmriegel, P., Pielichowski, J., and Pielichowski, K., 2003. "Carbazole containing polymers: Synthesis, properties and applications." *Prog. Polym. Sci.*, vol. 28, pp. 1297–1353.
- [17] Morin, J. F., Leclerc, M., Adès, D., and Siov, A., 2005. "Review : Polycarbazoles: 25 years of progress, macro molec." *Rapid Commun*, vol. 26, pp. 761-778.
- [18] Rejania, P. and Beenab, B., 2013. "Structural and optical Properties of polyindole-manganese oxide nanocomposite." *Ind. J. of Adv. in Chem. Sci.*, vol. 2, pp. 244-248.
- [19] Kavanoz, M. and Kilic, G., 2015. "Synthesis and characterization of polycarbazole-polyaniline copolymer in dichloromethanesolution." *J. of Turkish Chem. Soc.*, vol. 2, p. 33.
- [20] Alem, S., Graddage, N., Lu, J., Kololuoma, T., Movileanu, R., and Tao, Y., 2018. "Flexographic printing of polycarbazole-based inverted solar cells." *Org. Electron.*, vol. 52, pp. 146–152.
- [21] Nayana, V., Kanda, Kanda, S., and Subramina, B., 2020. "Polycarbazole and its derivative; progress synthesis and application." *J. Phys. Sci. Res.*, vol. 27, p. 285.
- [22] Lakard, S., Contal, E., Mouglin, K., and Lakard, B., 2022. "Electrodeposition and characterization of conducting polymer films Obtained from carbazole and 2-(9H-carbazol-9-yl)acetic acid." *Electrochem*, vol. 3, pp. 322–336.
- [23] Alberti, G., Cherubini, F., and Palombari, R., 1996. "Preparation, proton transport and use in gas sensors of thin film zirconium phosphate with γ -layered structure." *Sensors and Actuators*, vol. 1, pp. 179-183.
- [24] Albeti, G. and Torracca, E., 1968. "Synthesis of crystalline zirconium and titanium phosphate by direct precipitation." *J. Inorg. Nucl. Chem*, vol. 30, p. 320.

- [25] Clearfield, A., 1982. *Inorganic ion exchange materials*. Boca Raton: CRC Press, FL.
- [26] Shakshooki, S. K., Naqvi, N., Kowalczyk, J., Khalil, S., Rais, M., and Tarish, F., 1988. "React." *Poly*, vol. 7, pp. 221-226.
- [27] Vecchio, S., Di-Rocco, R., and Ferragina, C., 2007. "Intercalation compounds of γ -zirconium and γ -titanium phosphates 1,10-phenantroline copper complex materials." *Themochimica Acta*, vol. 453, pp. 105-112.
- [28] Szirtes, L., Poko, Z., Shakshooki, S. K., Ahmed, M., Dehair, A., and Benhamed, A., 1989. *J. Therm. Anal.*, vol. 35, pp. 895-902.
- [29] Barganasco, C., Cambelli, F., Frezza, A., Galli, P., LaGinestra, A., and Turko, M., 1991. "Layered zirconium-tin phosphates." *Applied Catalysts*, vol. 1, pp. 155-68.
- [30] Trobajo, C. and Rodríguez, M. L., 1998. "Suárez, M. and, García,J.R., Layered mixed tin-titanium phosphates." vol. 13, p. 754759.
- [31] Shakshooki, S. K., Elakari, F. A., and Alahemmer, A. A., 2020. "Glassy-, α -Zirconium-Tin Phosphates / Fibrous Cerium(IV)phosphate-nanocomposite membranes self supported niline, its Co-pyrrole and co-indole polymerization agent." In *The 4th International conference Theories and Application Basic and Biosciences, J.Faculty of Science University of Misurata*. pp. 335-35.
- [32] Miguel, A., Salvadó, P. P., Camino, T., and José, G. R., 2007. "Crystal structure of cerium(IV)bis(phosphate) derivative." *J. Am. Chem. Soc.*, vol. 129, pp. 10970-10971.
- [33] Tushato, M., Danjo, M., Baba, Y., Murakom, M., and Nana, H., 1997. "Preparation and chemical properties of a novel layered cerium(iv) phosphate." *Bulletin of Chem. Soc. Jap.*, vol. 70, p. 143.
- [34] Shakshooki, S. K., Abuain, M. A., and El-Aouzi, A. M., 2015. "Nano fibrous eerium(IV) hydrogen phosphate membrane self supported aniline polymerization agent." *Amer. J. of Chem.*, vol. 5, pp. 67-74.
- [35] Romano, R. and Alves, O. S., 2005. "Fibrous cerium(iv) phosphate host of weak and strong Lewis bases." *Inclus. Phenom. and Macrocyclic*, vol. 51, p. 211.
- [36] Casciola, M., Costantino, U., and D'amico, S., 1988. "Ac Conductivity of cerium (iv) phosphate in hydrogen form solid state ionics." vol. 28, p. 617.
- [37] Hamann, C. H., Hamnet, A., and Vielstich, W., 1998. "Electrochemistry; wiley-vch; weinheim."
- [38] Hibbert, D. B., 1993. *Introduction to electrochemistry*. London: Macmillan Press LTD.
- [39] Kissinger, P. T. and Heineman, W. R., 1996. *Laboratory techniques in electroanalytical chemistry*. New York: Marcel Dekker.